CS 225A: Experimental Robotics
Homework 3

Name: Abhyudit Singh Manhas
SUID: 06645995

Problem 1

(a) We use the controller:

$$\begin{aligned} F &= \Lambda(-k_p(x - x_d) - k_v\dot{x}) \\ \Gamma &= J_v^T F + N^T(-k_{pj}(q - q_d) - k_{vj}\dot{q}) + g \end{aligned} \tag{1}$$

with gains

$$k_p = 100,\ k_v = 20,\ k_{pj} = 50,\ k_{vj} = 14 \tag{2}$$

The plot of the end-effector trajectory is shown below:

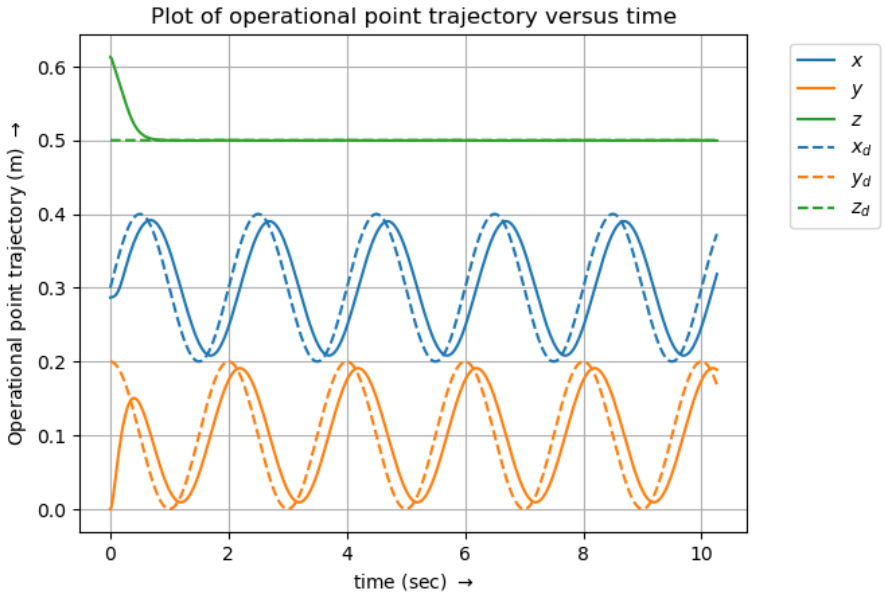

Figure 1: Plot of end-effector trajectories.

We can observe that the actual trajectory does not perfectly match the desired trajectory. This is because the above controller is better suited for the situation where the desired position is not time-varying, and is rather a constant (for example, moving the robot to a fixed position). However, this is not the case here, as the desired position is a function of time (trajectory tracking).

(b) We have

$$x_d(t) = \begin{bmatrix} 0.3 \\ 0.1 \\ 0.5 \end{bmatrix} + A \begin{bmatrix} \sin(\omega t) \\ \cos(\omega t) \\ 0 \end{bmatrix} \tag{3}$$

where $A = 0.1$ and $\omega = \pi$. Differentiating and double-differentiating 3 with respect to time gives:

$$\dot{x}_d(t) = A\omega \begin{bmatrix} \cos(\omega t) \\ -\sin(\omega t) \\ 0 \end{bmatrix} \tag{4}$$

and

$$\ddot{x}_d(t) = -A\omega^2 \begin{bmatrix} \sin(\omega t) \\ \cos(\omega t) \\ 0 \end{bmatrix} \tag{5}$$

(c) We now use the controller:

$$\begin{aligned} F &= \Lambda(\ddot{x}_d - k_p(x - x_d) - k_v(\dot{x} - \dot{x}_d)) \\ \Gamma &= J_v^T F + N^T(-k_{pj}(q - q_d) - k_{vj}\dot{q}) + g \end{aligned} \tag{6}$$

The plot of the end-effector trajectory is shown below:

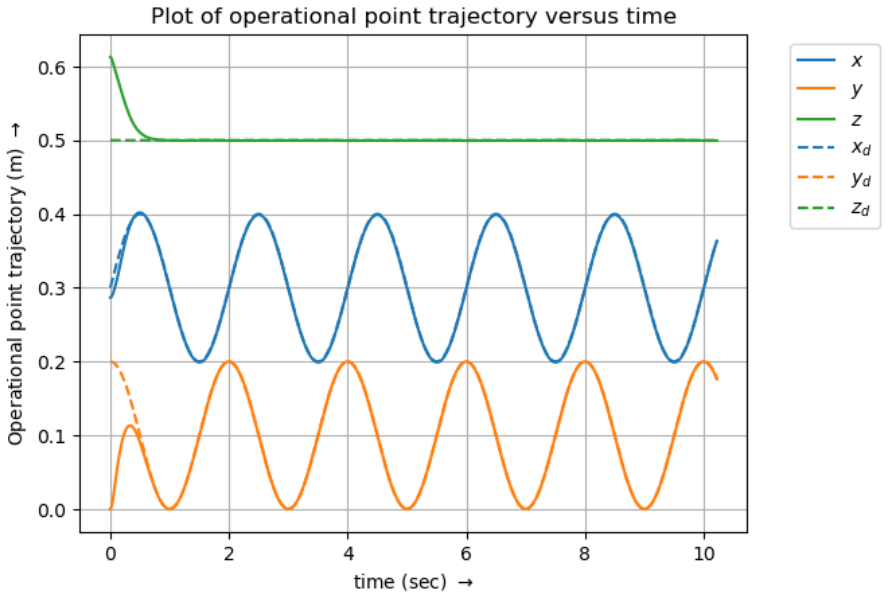

Figure 2: Plot of end-effector trajectories.

Compared to 1 (a), we now observe that the actual trajectory perfectly matches the desired trajectory. This is because, in addition to position and velocity feedback, the above controller also involves an acceleration feed-forward component that allows the system to better anticipate changes on the desired trajectory.

Problem 2

(a) We have:

$$V_{mid}(q) = k_{mid} \sum_{i=1}^{n} \left(q_i - \frac{\bar{q}_i + \underline{q}_i}{2} \right)^2 \tag{7}$$

From this, we can clearly see that:

$$\frac{\partial V_{mid}}{\partial q_i} = 2k_{mid} \left(q_i - \frac{\bar{q}_i + \underline{q}_i}{2} \right) \tag{8}$$

Hence, we have:

$$\nabla V_{mid} = \begin{bmatrix} \frac{\partial V_{mid}}{\partial q_1} \\ \frac{\partial V_{mid}}{\partial q_2} \\ \vdots \\ \frac{\partial V_{mid}}{\partial q_n} \end{bmatrix} = 2k_{mid} \begin{bmatrix} q_1 - \frac{\bar{q}_1 + \underline{q}_1}{2} \\ q_2 - \frac{\bar{q}_2 + \underline{q}_2}{2} \\ \vdots \\ q_n - \frac{\bar{q}_n + \underline{q}_n}{2} \end{bmatrix}$$

$$\implies \Gamma_{mid} = -\nabla V_{mid} = -2k_{mid} \begin{bmatrix} q_1 - \frac{\bar{q}_1 + \underline{q}_1}{2} \\ q_2 - \frac{\bar{q}_2 + \underline{q}_2}{2} \\ \vdots \\ q_n - \frac{\bar{q}_n + \underline{q}_n}{2} \end{bmatrix} = -2k_{mid}(q - \tilde{q}) \tag{9}$$

where $\tilde{q}_i = \frac{\bar{q}_i + \underline{q}_i}{2}$

(b) We have:

$$\begin{aligned} \Gamma_1 &= J_v^T F + N^T(-k_{pj}(q - q_d) - k_{vj}\dot{q}) + g \\ \Gamma_2 &= J_v^T F + N^T(\Gamma_{mid} + \Gamma_{damp}) + g \end{aligned} \tag{10}$$

where Γ_1 and Γ_2 correspond to command torques from problem 1 and 2 respectively.
We have from 10:

$$\Gamma_1 - \Gamma_2 = N^T(-k_{pj}(q - q_d) - k_{vj}\dot{q} - \Gamma_{mid} - \Gamma_{damp}) \tag{11}$$

For the same dynamic response, we should have:

$$\Gamma_{damp} = -k_{damp}\dot{q} = -k_{vj}\dot{q} \tag{12}$$

and

$$\Gamma_{mid} = -2k_{mid}(q - \tilde{q}) = -k_{pj}(q - q_d) \tag{13}$$

We can see from 12 and 13 that Γ_{damp} is responsible for joint damping in the null space of the control task, and Γ_{mid} is responsible for providing the required attraction to the mid-range joint positions of the manipulator, respectively.

(c) We have from 12:

$$k_{damp} = k_{vj} = 14 \tag{14}$$

Similarly we have from 13:

$$2k_{mid} = k_{pj} \implies k_{mid} = \frac{k_{pj}}{2} = 25 \tag{15}$$

(d) We use the controller:

$$F = \Lambda(-k_p(x - x_d) - k_v\dot{x})$$
$$\Gamma = J_v^T F + N^T \Gamma_{damp} + g \tag{16}$$

The plots of the end-effector trajectory, and joint trajectories for joints 4 and 6, are shown below:

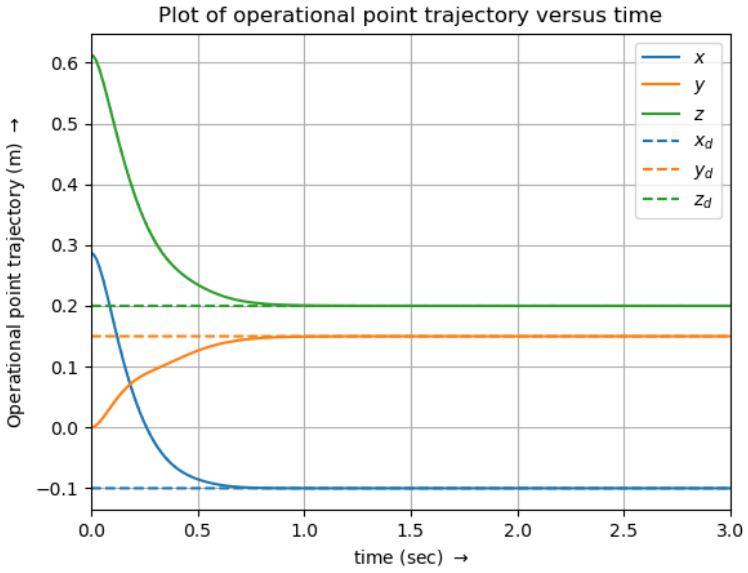

Figure 3: Plot of end-effector trajectories.

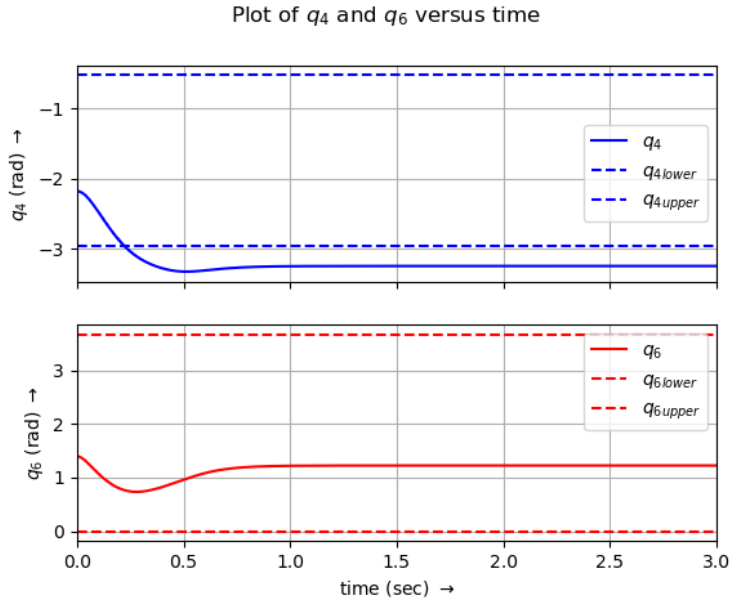

Figure 4: Plot of joint trajectories for joints 4 and 6.

We observe that we are able to track the desired end-effector position. We also see that joint 6 stays within its limits, but joint 4 violates and goes below its lower limit. This is because we have not yet added the potential field to avoid joint limits.

(e) We use the controller:

$$F = \Lambda(-k_p(x - x_d) - k_v\dot{x})$$
$$\Gamma = J_v^T F + N^T\Gamma_{mid} + N^T\Gamma_{damp} + g \tag{17}$$

The plots of the end-effector trajectory, and joint trajectories for joints 4 and 6, are shown below:

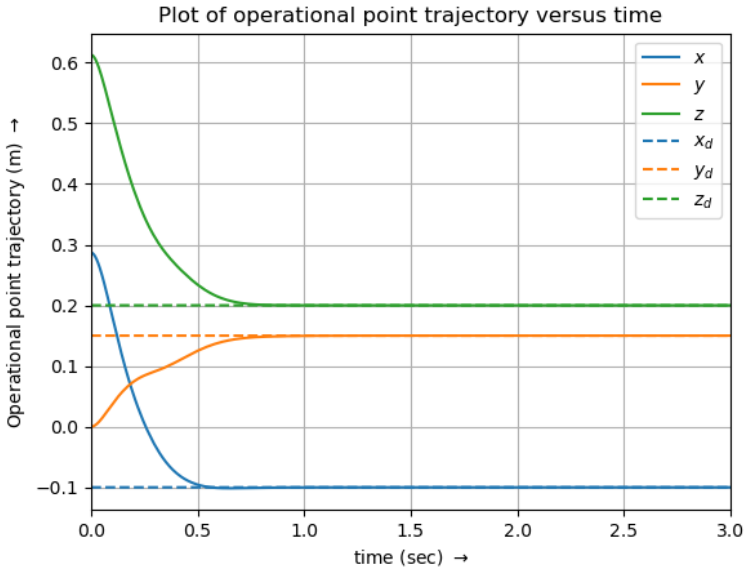

Figure 5: Plot of end-effector trajectories.

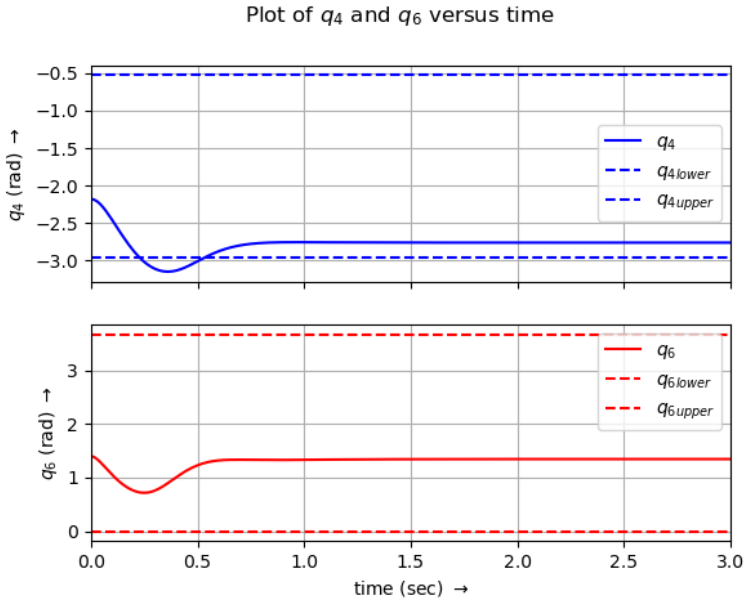

Figure 6: Plot of joint trajectories for joints 4 and 6.

We observe that we are able to track the desired end-effector position. Compared to 2 (d), now both joints 4 and 6 stay within their limits, with joint 4 being quite close to its lower limit. This is because we have now added the potential field to avoid joint limits.

(f) We use the controller:

$$F = \Lambda(-k_p(x - x_d) - k_v\dot{x})$$
$$\Gamma = J_v^T F + N^T\Gamma_{mid} + N^T\Gamma_{damp} + g \tag{18}$$

The plots of the end-effector trajectory, and joint trajectories for joints 4 and 6, are shown below:

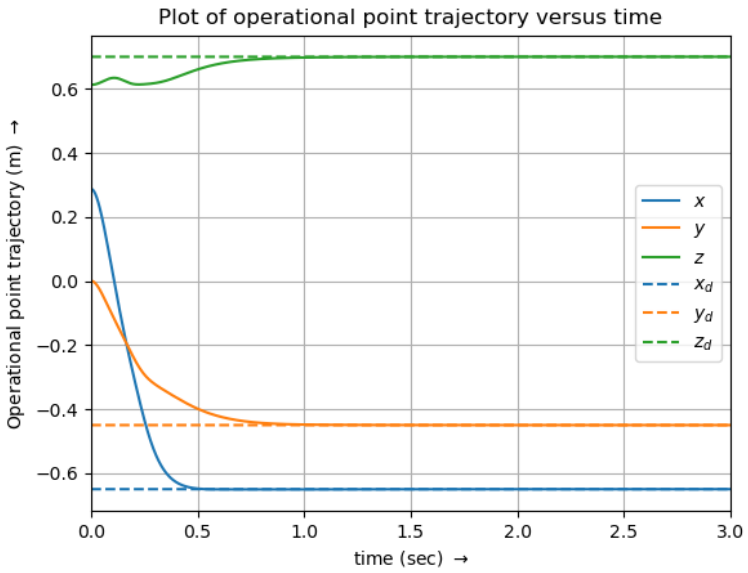

Figure 7: Plot of end-effector trajectories.

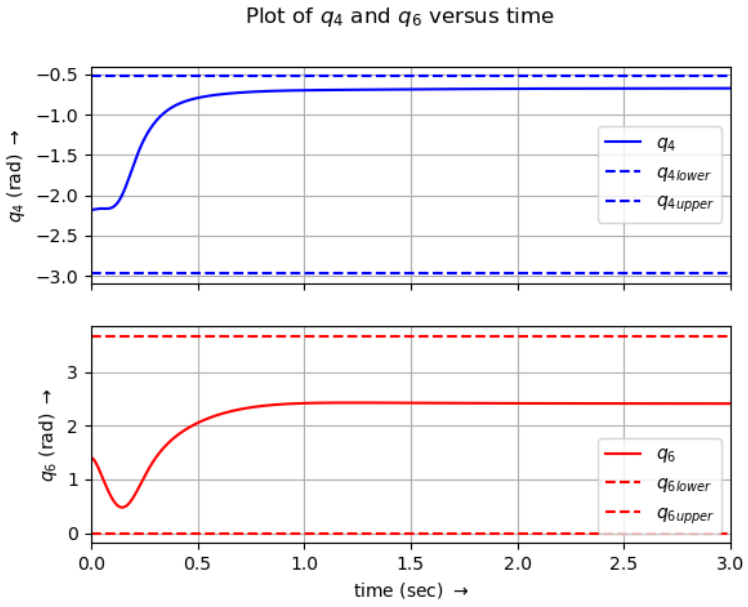

Figure 8: Plot of joint trajectories for joints 4 and 6.

We observe that we are able to track the desired end-effector position. We also see that both joints 4 and 6 stay within their limits (due to the added potential field), but compared to 2 (e), joint 4 is now

quite close to its upper limit. This is because the new end-effector position corresponds to the upper bound for joint 4, whereas the previous position corresponded to the lower bound.

(g) We use the controller:

$$F = \Lambda(-k_p(x - x_d) - k_v\dot{x})$$
$$\Gamma = J_v^T F + \Gamma_{mid} + N^T \Gamma_{damp} + g \tag{19}$$

The plots of the end-effector trajectory, and joint trajectories for joints 4 and 6, are shown below:

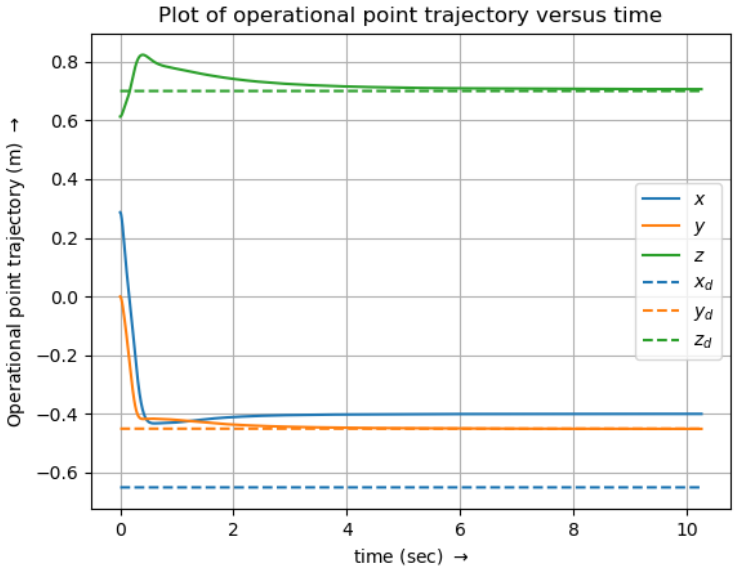

Figure 9: Plot of end-effector trajectories.

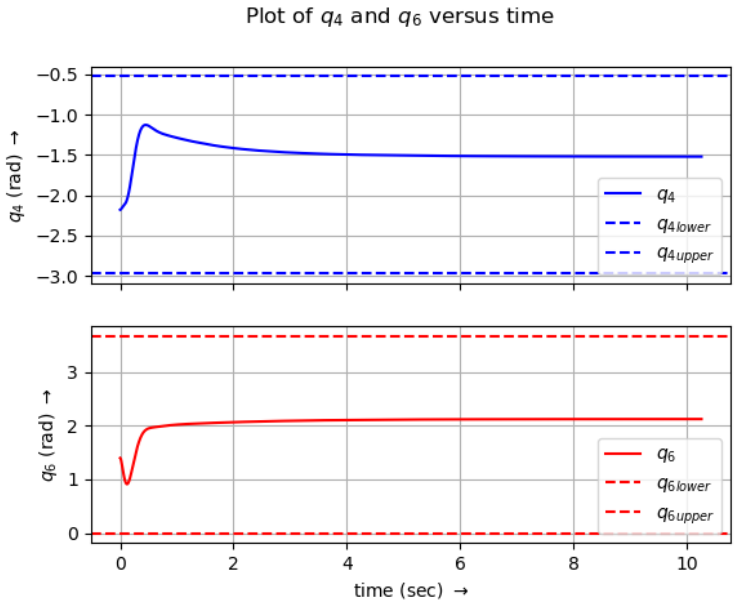

Figure 10: Plot of joint trajectories for joints 4 and 6.

Compared to 2 (f), we observe that now we are no longer able to track the desired end-effector position. However, both joints 4 and 6 stay well within their limits, and do not approach either limit. This is because Γ_{mid} (designed to avoid joint limits) is not projected onto the null space. This makes all joints approach their mid-range positions, but since Γ_{mid} now interferes with the end-effector dynamics, we are unable to track the desired end-effector position.
Between the controllers from part (f) and (g), I would prefer the one from part (f), as technically, all joints are within their limits in both the cases. So the only deciding factor is if we are able to track the desired end-effector position, which we are able to for part (f), but unable to for part (g).

Problem 3

(a) We implement the control law:

$$\begin{aligned} \delta\phi &= -\frac{1}{2}\sum_{n=1}^{3} R_i \times (R_d)_i \\ F &= \Lambda_0 \begin{bmatrix} -k_p(x - x_d) - k_v\dot{x} \\ -k_p\delta\phi - k_v\omega \end{bmatrix} \\ \Gamma &= \begin{bmatrix} J_v \\ J_\omega \end{bmatrix}^T F - N_0^T k_{vj}\dot{q} + g \end{aligned} \tag{20}$$

with gains:

$$k_p = 100,\ k_v = 20,\ k_{pj} = 50,\ k_{vj} = 14 \tag{21}$$

The plots of the end-effector trajectory and $\delta\phi$ are shown below:

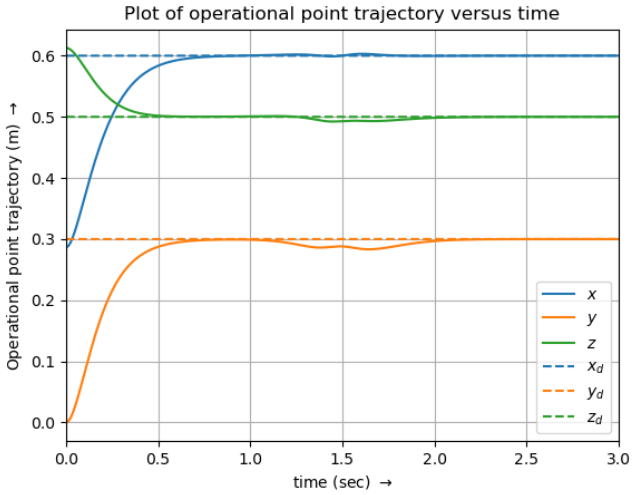

Figure 11: Plot of end-effector trajectories.

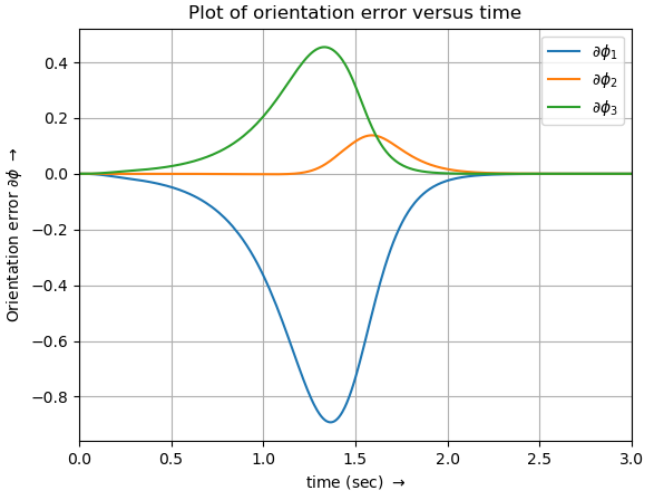

Figure 12: Plot of orientation error.

We observe that we are able to track the desired end-effector position. Also the orientation error eventually settles down to zero with time, indicating that the robot has been controlled to the desired orientation successfully.

Problem 4

(a) We implement the control law:

$$\begin{aligned} F &= \Lambda(-k_p(x - x_d) - k_v\dot{x}) \\ \Gamma &= J_v^T F + N^T M(-k_{pj}(q - q_d) - k_{vj}\dot{q}) + g \end{aligned} \tag{22}$$

For critical damping (with $k_p = 200$), our gains are:

$$k_p = 200,\ k_v = 2\sqrt{k_p} = 2\sqrt{200} \approx 28,\ k_{pj} = 50,\ k_{vj} = 14 \tag{23}$$

The plots of the end-effector trajectory and velocity are shown below:

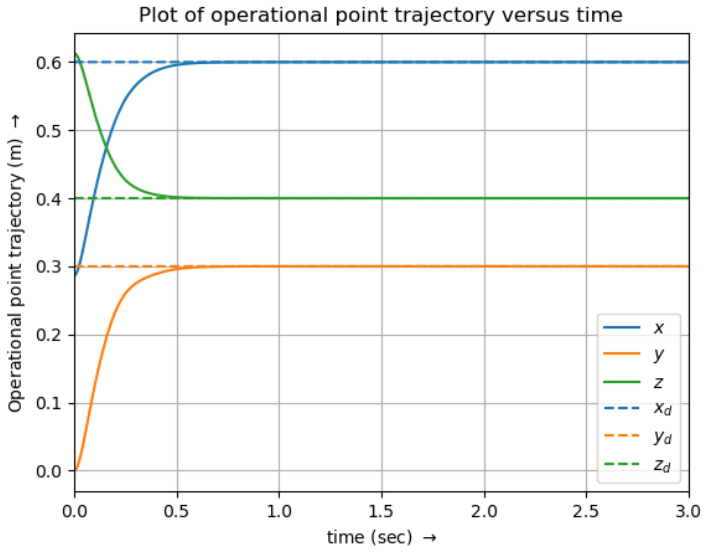

Figure 13: Plot of end-effector trajectories.

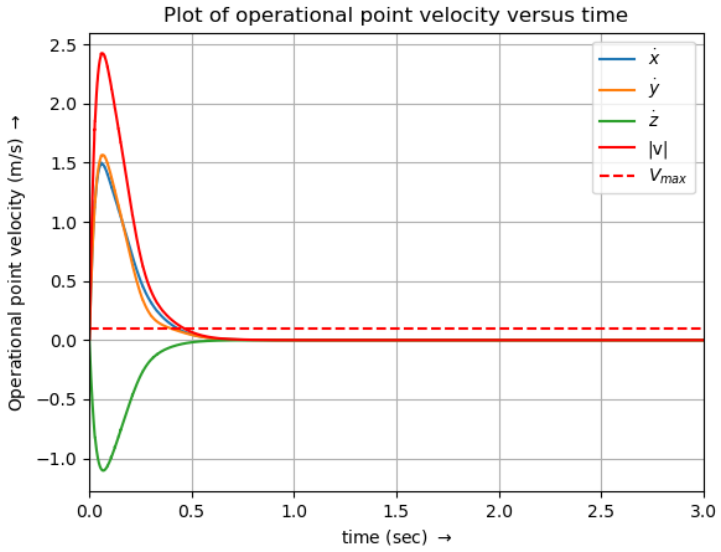

Figure 14: Plot of end-effector velocities.

In figure 14, $|v|$ is the magnitude of the end-effector velocity, that is:

$$|v| = \sqrt{\dot{x}^2 + \dot{y}^2 + \dot{z}^2} \tag{24}$$

We are able to track the desired end-effector position. Without velocity saturation, the robot moves quickly and $|v|$ exceeds V_{max} during the motion.

(b) We now implement velocity saturation with:

$$\begin{aligned} \dot{x}_d &= -\frac{k_p}{k_v}(x - x_d) \\ F &= \Lambda(-k_v(\dot{x} - \nu\dot{x}_d)) \\ \nu &= sat\left(\frac{V_{max}}{|\dot{x}_d|}\right) \end{aligned} \tag{25}$$

where $sat()$ is the saturation function:

$$sat(x) = \begin{cases} x & \text{if } |x| \leq 1.0 \\ sgn(x) & \text{if } |x| > 1.0 \end{cases} \tag{26}$$

and $sgn(x)$ is the sign function.
The plots of the end-effector trajectory and velocity are shown below:

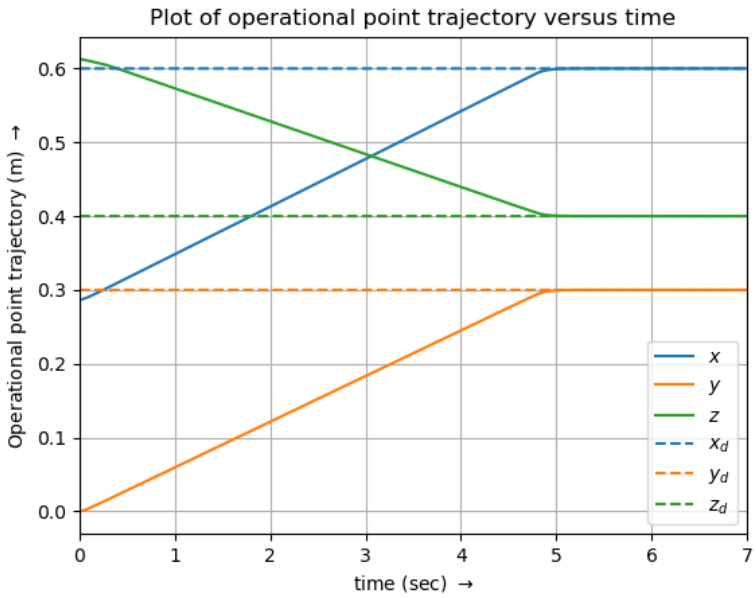

Figure 15: Plot of end-effector trajectories.

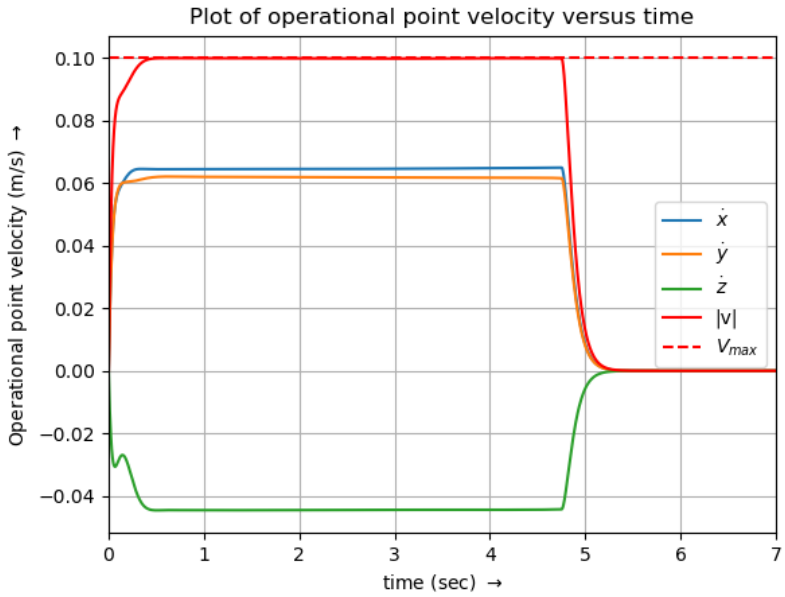

Figure 16: Plot of end-effector velocities.

We are able to track the desired end-effector position. Now with velocity saturation, the robot moves slowly and so takes a longer time to reach the desired position compared to 4 (a), but $|v|$ never exceeds V_{max} during the motion.